Journal of Visualized Experiments

Measurement of Pulse Propagation Velocity, Distensibility and Strain in an Abdominal Aortic Aneurysm Mouse Model --Manuscript Draft--

Article Type:	Invited Methods Article - JoVE Produced Video		
Manuscript Number:	JoVE60515R2		
Full Title:	Measurement of Pulse Propagation Velocity, Distensibility and Strain in an Abdom Aortic Aneurysm Mouse Model		
Section/Category:	JoVE Immunology and Infection		
Keywords:	Abdominal aortic aneurysm, animal models of human disease, pulse propagation velocity, distensibility, strain, aortic stiffness, in-vivo imaging		
Corresponding Author:	Chetan P. Hans University of Missouri Columbia Columbia, MO UNITED STATES		
Corresponding Author's Institution:	University of Missouri Columbia		
Corresponding Author E-Mail:	HansCP@health.missouri.edu		
Order of Authors:	Chetan P. Hans		
	Neekun Sharma		
	Zhe Sun		
	Michael A Hill		
Additional Information:			
Question	Response		
Please indicate whether this article will be Standard Access or Open Access.	Standard Access (US\$2,400)		
Please indicate the city, state/province, and country where this article will be filmed . Please do not use abbreviations.	Columbia, MO, USA		

UNIVERSITY of MISSOURI

DALTON CARDIOVASCULAR RESEARCH CENTER

OFFICE OF RESEARCH

Jaydev Upponi Science Editor Immunology and Infection Editorial Department JoVE September 3, 2019,

Dear Dr. Upponi,

Please find enclosed our revised manuscript entitled "High Frequency Ultrasound Evaluation of Abdominal Aortic Aneurysms in Angiotensin II-Induced Mouse Models" for potential publication in the JOVE.

In the present study, we have all the concerns raised by the Editor with regard to the highlighted steps, resolution of images and significance of using a notch inhibitor. We have also revised the figures and table of materials appropriately.

We hope that the revised article is suitable for publication in the JOVE.

Thank you for your consideration of this paper for potential publication.

Sincerely,

Chetan P. Hans, PhD

Assistant Professor

School of Medicine - Cardiology & Medical Pharmacology and Physiology &

Dalton Cardiovascular Research Center

University of Missouri

134 Research Park Drive

Columbia, MO 65211

573-884-7225 ph 573-884-4232 fx

HansCP@health.missouri.edu



1 TITLE:

2 Measurement of Pulse Propagation Velocity, Distensibility and Strain in an Abdominal Aortic

Aneurysm Mouse Model

4 5

3

AUTHORS AND AFFILIATIONS:

Neekun Sharma^{1,3*}, Zhe Sun^{1,2*}, Michael A. Hill^{1,2,3}, Chetan P. Hans^{1,2,3}

6 7

- 8 ¹Division of Cardiovascular Medicine, University of Missouri, Columbia
- 9 ²Medical Pharmacology and Physiology, University of Missouri, Columbia
- 10 ³Dalton Cardiovascular Research Center, University of Missouri, Columbia

11

*These authors contributed equally.

13

- 14 Correspondence to:
- 15 Chetan P. Hans (HansCP@health.missouri.edu)

16

- 17 Email Addresses of Co-authors:
- 18 Neekun Sharma (sharmane@health.missouri.edu)
- Zhe Sun (sunzh@missouri.edu)Michael A. Hill (hillmi@missouri.edu)

21

22 **KEYWORDS**:

23 Abdominal aortic aneurysm, animal models of human disease, pulse propagation velocity,

24 distensibility, strain, aortic stiffness, in vivo imaging

2526

27

28

SUMMARY

This manuscript describes a detailed protocol for using high frequency ultrasound imaging to measure luminal diameter, pulse propagation velocity, distensibility and radial strain on a mouse model of abdominal aortic aneurysm.

293031

32

33

34

35

36

37

38

39

40

41

ABSTRACT

An abdominal aortic aneurysm (AAA) is defined as a localized dilation of the abdominal aorta that exceeds the maximal intraluminal diameter (MILD) by 1.5 times of its original size. Clinical and experimental studies have shown that small aneurysms may rupture, while a subpopulation of large aneurysms may remain stable. Thus, in addition to the measurement of intraluminal diameter of the aorta, knowledge of structural traits of the vessel wall may provide important information to assess the stability of the AAA. Aortic stiffening has recently emerged as a reliable tool to determine early changes in the vascular wall. Pulse propagation velocity (PPV) along with the distensibility and radial strain are highly useful ultrasound-based methods relevant for assessing aortic stiffness. The primary purpose of this protocol is to provide a comprehensive technique for the use of ultrasound imaging system to acquire images and analyze the structural and functional properties of the aorta as determined by MILD, PPV, distensibility and radial strain.

42 43 44

INTRODUCTION

An abdominal aortic aneurysm (AAA) represents a significant cardiovascular disease characterized by a permanent localized dilation of the aorta exceeding the original vessel diameter by 1.5 times¹. AAA ranks among the top 13 causes of mortality in the United States². The progression of AAA is attributed to the degeneration of the aortic wall and elastin fragmentation, ultimately leading to aortic rupture. These changes in the aortic wall may occur without a significant increase in the maximal intraluminal diameter (MILD), thus suggesting that MILD alone is not sufficient to predict the severity of the disease³. Therefore, additional factors need to be identified to detect initial changes in the aortic wall, which may guide early treatment options. The overall goal of this protocol is to provide a practical guide for assessing aortic functional properties using ultrasound imaging as characterized by measurements of pulse propagation velocity (PPV), distensibility and radial strain.

A well characterized experimental model to study AAA, first described by Daugherty and colleagues, involves subcutaneous infusion of angiotensin II (AngII) via osmotic pumps in *Apoe*-/-mice⁴. Precise measurement of MILD using ultrasound imaging has been instrumental in characterizing AAA in this mouse model⁵. Although histological changes during the development of AAA have been extensively studied, changes in the functional properties of the vessel wall such as aortic stiffness have not been well characterized. This protocol emphasizes the use of high-frequency ultrasound in combination with the sophisticated analyses as powerful tools for studying the temporal progression of AAA. Specifically, these approaches allow us to assess the functional properties of the vessel wall as measured by PPV, distensibility and radial strain.

Recent clinical studies in human subjects with AAA, as well as in the murine elastase-induced AAA model, suggest a positive correlation between aortic stiffness and aortic diameter^{6,7}. PPV, an indicator of aortic stiffness, is accepted as an excellent measurement for quantifying changes in stiffness in vessel wall^{6,8}. PPV is calculated by measuring the transit time of the pulse waveform at two sites along the vasculature, thus providing a regional assessment of aortic stiffness. We have recently demonstrated that increased aortic stiffness as measured by PPV, and at the cellular level as determined using atomic force microscopy, positively correlates with aneurysm development⁹. Further, the literature suggests that aortic stiffness may precede aneurysmal dilation and thus may provide useful information about regional intrinsic properties of the vessel wall during development of AAA¹⁰. Similarly, distensibility and strain measurements are the quantification tools to measure earlier changes of arterial fitness. Healthy arteries are flexible and elastic, whereas with increased stiffness and less elasticity, distensibility and strain is decreased. Here, we provide a practical guide and step by step protocol for the use of a highfrequency ultrasound system to measure MILD, PPV, distensibility and radial strain in mice. The protocol provides technical approaches that should be used in conjunction with the basic information provided by manuals for specific ultrasound imaging instruments and the accompanying video tutorial. Importantly, in our hands the described imaging protocol provides reproducible and accurate data that appear valuable in the study of the development and progression of experimental AAA.

To further demonstrate the utility of ultrasound imaging, we provide example images and measurements taken from our own studies aimed at using pharmacological approaches for

preventing experimental AAA¹¹. Specifically, notch signaling has been proposed to be involved in multiple aspects of vascular development and inflammation¹². Using gene haploinsufficiency and pharmacologic approaches, we have previously demonstrated that Notch inhibition reduces the development of AAA in mice by preventing infiltration of macrophages at the site of vascular injury¹³⁻¹⁵. For the current article, using the pharmacological approach for Notch inhibition we focus on the relationship between aortic stiffness and factors relating to AAA. These studies illustrate that Notch inhibition reduces aortic stiffness, which is a measure of AAA progression¹¹.

96 97

PROTOCOL

98 99

100

The protocol for handling of mice and ultrasound imaging was approved by the University of Missouri Institutional Animal Care and Use Committee (animal protocol number 8799) and was conducted according to AAALAC International Standards.

101102103

1. Equipment setup and preparation of mice

104

105 1.1. Equipment setup

106

1.1.1. Turn on the ultrasound instrument, ultrasonic gel warmer and the heating pad.

108

1.1.2. Open the ultrasound program and enter the study name and descriptive information for each mouse.

111

112 1.1.3. Select the application as **General Imaging**.

113

1.1.4. Choose the appropriate transducer for abdominal imaging (**Figure 1B,C**). In this experiment, MS400 transducer is used.

116

1.1.5. Ensure anesthesia isoflurane and oxygen levels are adequate for each experimental session.

119

120 1.1.6. Clean the ultrasound animal imaging platform.

121

122 1.2. Mouse preparation

123

1.2.1. Place the mouse cage on top of a heating pad (36.5 to 38.5 °C).

125

1.2.2. Gently hold the mouse by its tail and place in the oxygen-filled isoflurane chamber.

127

128 1.2.3. Direct the isoflurane and oxygen flow to the induction chamber.

129

130 1.2.4. Turn on the isoflurane vaporizer and set the isoflurane level to 1-2% vol/vol. Turn on the oxygen tank pressure to 1-2 L/min.

132

133 1.2.5. After ~2 min, confirm the adequate depth of anesthesia by the absence of withdrawal reflexes upon pinching the foot pad of the mouse.

135

136 1.2.6. Next, turn off the induction chamber supply branch and turn on the branch directed to the anesthesia nose cone.

138

139 1.2.7. Transfer the mouse from the induction chamber to the ultrasound imaging stage and position the anesthesia cone over the nose of the animal.

141

1.2.8. Tilt the animal imaging platform around 10° to the lower right corner for optimal scanning (Figure 1B).

144

1.2.9. Put one drop of sterile ophthalmic solution in both eyes of mice to prevent drying under anesthesia.

147

148 1.2.10. Position the mouse in the supine position with its nose inserted into the anesthesia cone.

149

150 1.2.11. Apply the electrode gel to all four paws using a cotton swab and tape the paws to the copper leads on the animal imaging platform for electrocardiogram readings (Figure 1C).

152

153 1.2.12. Use clippers to shave hair at the imaging site and then apply depilatory cream to remove remaining fur. Leave for less than 1 min.

155

1.2.13. Gently wipe off the cream and hair with a damp paper towel.

156157158

1.2.14. Monitor the breathing and ensure that heart rate is maintained between 450-550 beats/min. If below this level, reduce the isoflurane flow and wait until the heart rate recovers.

159160

161

1.2.15. Apply prewarmed ultrasonic gel (37 °C) to the prepared skin site and attach the transducer to its holder and lower down until it touches the gel (Figure 1C).

162163164

2. Ultrasound imaging of the abdominal aorta

165

2.1. Position the transducer horizontally (i.e., perpendicular to the midline of the mouse).

168

169
 170 2.3. Lower the transducer and place 0.5 - 1 cm below the diaphragm after touching the gel. Now
 171 start to observe the images.

2.2. Smooth the ultrasonic gel and remove bubbles using the wood stick of a cotton swab.

172

2.4. Visualize the abdominal aorta in the short axis view (**Figure 1C**).

174

NOTE: B-mode is the default and most effective mode to anatomically locate the aorta and position the transducer. The abdominal aorta is identified by the presence of pulsatile flow using

color Doppler and power Doppler modes in the short axis (i.e., the circumferential cross-section of the aorta). Adjust the micromanipulators on the animal stage and the transducer to bring the cross section of the aorta to the center of the image.

2.5. Gently rotate the transducer 90° clockwise, and slowly adjust the x-axis micromanipulator knob to visualize the aorta in long axis view (longitudinal section of the aorta).

 NOTE: In many cases, gastro-intestinal gases may interfere with the image, or the aorta may not be at the optimal angle to allow a clear long axis view. Adjust the angle of the transducer slowly and horizontally until an acceptable long axis view is obtained. If problems persist, elevate the transducer, check for air bubbles under the transducer, slightly adjust the tilting angle of the animal stage, reapply gels, and repeat all the steps again.

2.6. Set the focus zone and depth at the region of the aorta using the **Focus Zone** and **Focus Depth** toggles, respectively. Adjust the **time gain compensation slider** manually to darken the lumen of the aorta to achieve an optimal contrast of the aorta wall.

2.7. Adjust the **y-axis manipulator** to visualize the branching points of the superior mesenteric and the right renal arteries. Use the right renal artery as a landmark to capture image of the suprarenal aorta (**Figure 2A**).

2.8. Record at least 100 frames of B-mode images on the suprarenal aorta.

2.9. Press cinestore to save the B-mode images.

2.10. Press **M-mode** button on the instrument keyboard to enable M-mode recording. Roll the cursor ball to bring the yellow indicator line to a normal aorta sections with clear vessel wall image, or to the sections where maximal diameter of aneurysm is observed.

2.11. Press the **SV/gate toggle** and adjust the cursor ball to ensure that vessel walls are included in the measurement bracket. Press **update** to record M-mode measurements and press **cinestore** to capture **(Figure 2A,B)**.

NOTE: Maximal diameter of the aneurysm may not be in the same imaging plane as the optimal long axis view of the aorta. Adjust the x-axis manipulator knob slightly for each M-mode measurement to ensure that the MILD of each section is captured.

2.12. To obtain ECG-gated Kilohertz Visualization (EKV) images, press the **B-mode** button to go back to B-mode recording.

NOTE: If the images are not sharp, adjust the x-axis manipulator to achieve the sharpest image of upper wall of the lumen over a section length (i.e., > 6 mm).

2.13. Press **Physio Settings** button on the keyboard and select **Respiration Gating**. Adjust the gating **Delay** and **Window** manually to record the data only during the flatter parts of the respiration wave. The recording sections will be shown as colored blocks on the tracing of the respiration wave.

224225

NOTE: Without the adjustment of the respiration gating, the EKV images will be blurred due to the normal movement of animal during breathing.

226227228

229

230

2.14. Press **EKV button** to enable the EKV mode. In the appropriate menu, select **Standard Resolution** and **frame rate 3000 or higher**. Select proceed to record **EKV images**. Press **cinestore** to save the images. Use EKV mode image to obtain measurements of pulse propagation velocity (PPV), distensibility and radial strain.

231232

NOTE: EKV recording may fail if there are abnormal fluctuations in respiration, animal is respiring too rapidly, or frame rates settings are too high. In those case, set the frame rate lower and wait for the animal respiration to stabilize. Setting the frame rate at 3000 is usually appropriate for both mice and rats.

237238

3. Post-imaging steps

239

3.1. Gently wipe the ultrasonic gel from the abdominal area of the mouse with a paper towel moistened with warm water.

242

3.2. Place the mouse back in its home cage on a heating pad.

244

3.3. Turn off the isoflurane machine, clean the animal imaging platform and transducer withdamp wipes.

247

3.4. Transfer the image data collected during the ultrasound scan to the hard drive.

249

3.5. Turn off the ultrasound instrument.

251

3.6. After the mouse recovers from anesthesia and is alert, remove the heating pad and returnthe cage to the animal housing rack.

254255

4. Analysis of abdominal aortic images

256257

4.1. Analysis of M-mode images to measure MILD

258

259 4.1.1. Open the ultrasound program and enter the study name and descriptive information for each mouse.

261

262 4.1.2. Open the ultrasound data in the analysis software and open the M-mode image and pause the heartbeat.

264265 4.1.3. Click on Measurements.

4.1.4. Select the **vascular package** from the drop-down options. Click on **Depth** and draw a line across the aortic lumen extending from inner wall to wall (**Figure 2C,D**).

NOTE: For consistency, the measurements should be taken at the systolic phase of the cardiac cycle when the aorta is maximally expanded. Draw three lines across three different heartbeats to obtain accurate and average measurements of MILD. In AAA, the measurements are taken at the maximal dilatation of the aorta. It is also advisable to fast the animals 4-6 h prior to collecting images to avoid interference from bowel motility and ensure image clarity.

4.2. Analysis for pulse propagation velocity (PPV)

4.2.1. Open the EKV image and pause the heartbeat.

4.2.2. Open a new window on the analysis software (e.g., Vevo Vac) by clicking on the name icon.

4.2.3. Click on the **PPV option (arrow in Figure 3D)**. A small window will further appear with the image of the aorta.

4.2.4. Draw a rectangular box by clicking on the upper vessel wall and dragging the pointer for about 4 mm covering both the walls of the suprarenal aorta.

NOTE: Keep the length of the box consistent (~4 mm) for all the images. The user can adjust the rectangular box by rotating to align the box and selecting the line then dragging to a new position on the vessel being analyzed to obtain the most appropriate and clear inflection of the pulse wave. The vertical lines of data from the rectangle will be displayed and identified as the Left (top image) and Right (bottom image) on the ROI. For a better visualization of the inflection of the pulse wave, it is sometimes useful to the draw box only on the upper wall as shown in **Figure 3**. The software will automatically calculate the PPV (m/s). However, it's always better to manually adjust the purple lines to set the exact inflection point on the pulse waves and PPV will change accordingly.

4.2.5. Finally, select the **Accept** command to save the PPV values. Export the figures and the data to the data storage drive.

4.3. Analysis for distensibility and radial strain

4.3.1. Open the EKV image and pause the heartbeat.

4.3.2. Click on the software icon. The software will open a new window.

 4.3.3. Click on the **trace new ROI** and draw a rectangular box on the both walls of the vessel. The software will automatically trace the upper and lower walls of the vessel. The user can adjust the trace to align on the wall by clicking on green points (**Figure 4A,B**).

4.3.4. Now **Accept** the trace. The software will calculate the distensibility (1/Mpa) in the selected ROI.

4.3.5. For the radial strain measurement, select the appropriate strain option from the menu bars on the top left. The images for radial strain and tangential strain will open.

4.3.6. Obtain the value for radial strain (%) by moving the cursor on the peak of the curve. Export the data as images or in video format (Figure 4A,B).

REPRESENTATIVE RESULTS

Representative M-mode images of the normal and aneurysmal abdominal aorta from mice are shown in **Figure 2A** and **Figure 2B**, respectively. The suprarenal abdominal aorta is identified by its location next to right renal artery and the superior mesenteric artery (**Figure 2A**). Representative images used for the calculation of MILD, at three different heartbeats of the systolic cardiac cycle, in normal and aneurysmal aorta are shown in **Figure 2C,D** respectively. In the situation where an aortic aneurysm has developed, the luminal diameter is determined by drawing a perpendicular yellow line between the two inner edges of the lumen at the area of maximal dilation (**Figure 2B**). Three independent measurements are typically averaged to determine an accurate intraluminal diameter.

Representative EKV images of the abdominal aorta used in analysis of PPV are shown in **Figure 3**. PPV is calculated by drawing a rectangular box on the luminal wall of suprarenal aorta (**Figure 3E**) and adjustment of the purple vertical lines of data obtained from the rectangular box (**Figure 3F**). The purple lines should be adjusted to set the inflection point of the pulse waves. Representative EKV images of the abdominal aorta suitable for analysis of distensibility and radial strains are shown in **Figure 4**. Distensibility and radial strain are calculated by tracing the luminal walls of the suprarenal aorta as shown in **Figure 4E**. The value for distensibility (1/MPa) is obtained by choosing the distensibility/elasticity option from drop down menu of the box (red arrow, **Figure 4F**). The radial strain (%) is obtained by choosing the radial strain option (**Figure 4G**) and moving the cursor to the peak of the radial strain graph (**Figure 4H**).

We have validated the significance of PPV in the AngII-induced mouse model of AAA and further examined the therapeutic potential of a Notch inhibitor (N-[N-(3,5-difluorophenacetyl)-L-alanyl]-(S)-phenylglycine t-butyl ester; DAPT) on the progression and stability of pre-established AAA. Specifically, all these aneurysm studies were performed on 8-10 weeks old *Apoe-/-* male mice following infusion of AngII by published protocols^{4,13}. At day 28 of AngII infusion, mice were randomly divided into two groups and were administered vehicle or DAPT (10 mg/kg) until sacrifice at day 56¹³. Transabdominal ultrasound imaging showed a progressive increase in the MILD, PPV, and a decrease in distensibility and radial strain in response to AngII at day 28 (**Figure 5A-E**). AngII infusion marginally increased MILD from day 28 to 56 and DAPT did not significantly

change MILD compared to AnglI alone (**Figure 5A** and **Figure 5B**). However, PPV increased progressively with AnglI infusion at from day 28 to day 56 and DAPT significantly decreased further increases in PPV at day 56 (**Figure 5C**). Distensibility and radial strains, parameters to assess the elasticity of the vessel wall were decreased with AnglI infusion while DAPT showed no significant effect (**Figure 5D** and **5E**). It is important to appreciate that PWV correlated strongly with MILD at day 28 (R²=0.51, **Figure 5F**), whereas at day 56, the correlation was relatively weak (R²=0.22) (**Figure 5G**). Aortic stiffness in AAA is primarily associated with changes in aortic wall architecture. Histologically, AnglI infusion increased collagen degradation and proteolytic activity in the medial layer of the aorta (**Figure 5H**, **top row**). DAPT treatment minimized such changes in the ECM degradation (**Figure 5H**, **bottom row**).

FIGURE LEGENDS

Figure 1: Setup of the instrument. (A) Overall view of the ultrasound machine along with induction chamber for anesthesia and gel warmer. **(B)** Close up view of the imaging platform and the transducer system. **(C)** The view of the transducer placement while capturing short axis image of the abdominal aorta.

Figure 2: Analysis of M-mode images for obtaining maximal intraluminal diameter (MILD). The M-mode images of normal aorta (A) and aorta with abdominal aortic aneurysm (B) from mice are shown. (C) and (D), MILD drawn at systolic phase of the cardiac cycle in the suprarenal aorta of normal mice (C) and mice with AAA (D). Measurements at three different heartbeats are taken as shown and the average value is calculated.

Figure 3: Analysis of EKV images for obtaining pulse propagation velocity (PPV). EKV images collected from normal mouse aorta. Analysis is done by clicking on measurements (**A**) and the software icon (**B**). A new window will appear with the icons on the right side, as shown in **C**. Now, click on PPV (**D**) and again, a small window will appear (**E**). Draw a rectangular box on the upper wall of the lumen as shown in **E** and click accept. The PPV value will be obtained as shown in **F** (arrow). The purple lines is adjusted to set the inflection point of the pulse waves (**G**).

Figure 4: Measurement of distensibility and radial strain. EKV images collected from normal mouse aorta. Analysis is done by clicking on measurements (A) and the software icon (B). A new window will appear with the icons on the right side, as shown in C. Now, click on trace new ROI (D), a new window will appear with traces on the upper and the lower wall of the lumen as shown in E and click accept. The value for distensibility will be obtained in table as show in the F. For strain, click on strain (G). The window will show the radial strain value (%, green highlighted box), as the cursor is placed on the peak of the radial strain graph (H).

Figure 5. PPV correlates with structural traits of aorta in the established AAA. (A) Representative transabdominal ultrasound images showing the MILD at day 0, 28, 42 and 56 of indicated experimental groups in *Apoe*-/- mice. DAPT was started at day 28. Dotted yellow lines outline the lumen. (B) Quantification of MILD in the indicated groups (purple and green color shows AngII + vehicle and AngII + DAPT treated mice respectively (n=16-18). (C, D and E) PPV, distensibility and

radial strain at various days of AngII and DAPT treatments (n=8). (**F and G**), Graphs showing Pearson's correlation between PPV and MILD at day 28 (**F**) and day 56 (**G**). (**H**) Representative histological images for collagen staining (stained with trichrome and seen as blue staining) and proteolytic activity by in situ zymography with or without DAPT treatment at day 56. Tukey multiple comparisons test was used for data analysis. *P<0.05; ns = non-significant. Scale 50 μ m in H. This figure is adapted from Sharma et al. (2019), Scientifc Reports (SREP-19-16491B)¹¹.

DISCUSSION

Ultrasound imaging provides a powerful technique for determining functional properties of the aorta through measurements of PPV, distensibility and radial strain. These measurements are particularly instructive for studying mouse models of AAA and the in vivo approach allows for collection of longitudinal data that is potentially important to understanding temporal development of the aortic pathology. Specifically, measurements of in vivo aortic stiffness are determined locally in the abdominal aorta by PPV, distensibility and radial strain by analyzing EKV data and are considered as an independent risk factor for AAA instability¹⁶. The techniques described in these protocols are relatively straight forward and take only 8-10 min to obtain image sets from one mouse. All images should preferably be collected by a single operator using well-defined and consistent landmarks to generate reproducible and precise data.

There are potential factors that require technical expertise for the applications of these tools. For example, firstly, PPV may not solely reflect the degree of AAA development in the local arterial wall because it is an indirect measure of regional arterial stiffness. Secondly, it can be difficult to accurately measure PPV if the intimal wall is damaged. Third, it can be challenging to obtain sharp resolution images without expertise in operating the instrument. Some of these concerns have been addressed in recent versions of ultrasound imaging systems where speckle noise and artifacts are reduced, while preserving and enhancing data acquisition for small animal studies.

The focus of techniques used in the past (Doppler, microangiography, magnetic resonance imaging) to determine aortic stiffness were limited to two-dimensional images. PPV calculated from the ultrasound imaging has been emerging as a reliable and reproducible method to determine aortic stiffness and seems to be independent of arterial pressure^{9,17}. It is important to note that the prevailing definition of AAA using maximal diameter as a standard index does not always reliably correlate with clinical observations. For instance, small aneurysms may rupture while some large aneurysms tend to remain stable¹⁸⁻²⁰. Aortic stiffening is an early change generating aortic wall stress that triggers aneurysmal growth, and remodeling¹⁰ and has been strongly correlated with Mmp2 and Mmp9 in mouse models of AAA¹⁰. Thus, in addition to the diameter of the aorta, functional analyses may provide important information to assess the progression and stability of AAA.

Using these protocols, we have examined the therapeutic potential of a potent pharmacological Notch inhibitor (2S-N-[(3,5-Difluorophenyl) acetyl]-L-alanyl-2-phenylglycine 1,1-dimethylethyl ester; DAPT) on the progression and stability of pre-established AAA using an AnglI-induced mouse model of AAA¹¹. Transabdominal ultrasound imaging showed a progressive increase in the MILD, PWV, and a decrease in distensibility and radial strain in the *Apoe*-/- mice in response to

439 Angli than controls at day 28. No further increase in MILD was observed beyond day 28 till day 440 56 (Figure 5). However, PPV increased progressively and was significantly higher at day 56 441 compared to day 28. With the inhibition of Notch signaling by DAPT, MILD mice was not 442 significantly different from AnglI alone at day 56. Interestingly, DAPT prevented further increase in PPV such that it was significantly lower than AnglI at day 56 (Figure 5C). DAPT treatment did 443 444 not significantly affect distensibility or radial strain (Figure 5D,E). Interestingly, PPV correlated 445 strongly with MILD at day 28 (R^2 =0.51), whereas at day 56, the correlation was relatively weak 446 (R²=0.22; **Figure 5F**). These changes in the aortic stiffness were reflected in the increased collagen 447 degradation and proteolytic activity with AnglI and the attenuation by DAPT (Figure 5H). This 448 example study highlights the potential value of ultrasound-based aortic stiffness measurments 449 in understanding the time-course and predictability of both AAA progression and stability.

450 451

452

453

454

Further, the ultrasound based approach appears valuable in assessing the potential role for pharmacological interventions, particularly in stages that are likely to be independent of changes in intra-luminal diameter (i.e., beyond the expectation for actual regression). In summary, detailed understanding and usage of such technology will benefit in evaluating the prognosis of AAA at an early stage of the disease for effective therapeutic interventions.

455 456 457

ACKNOWLEDGMENTS

This work was supported by R01HL124155 (CPH) and funding from the Research Institute at the University of Missouri to CPH.

459 460 461

458

DISCLOSURES

The authors have nothing to disclose.

462 463 464

REFERENCES

- 465 1. Wanhainen, A. How to Define an Abdominal Aortic Aneurysm Influence on Epidemiology and Clinical Practice. *Scandinavian Journal of Surgery*. **97**, 105-109 (2008).
- 467 2. Benjamin, E. J. et al. Heart Disease and Stroke Statistics—2018 Update: A Report From the American Heart Association. *Circulation*. **137**, e67-e492 (2018).
- 3. Xu, J., Shi, G-P. Vascular wall extracellular matrix proteins and vascular diseases. Biochimica et biophysica acta. **1842**, 2106-2119 (2014).
- 471 4. Daugherty, A., Manning, M. W., Cassis, L. A. Angiotensin II promotes atherosclerotic lesions and aneurysms in apolipoprotein E-deficient mice. *Journal of Clinical Investigation*. **105**,

473 1605-12 (2000).

- 474 5. Au Sawada, H. et al. Ultrasound Imaging of the Thoracic and Abdominal Aorta in Mice 475 to Determine Aneurysm Dimensions. *Journal of Visualized Experiments*. e59013 (2019).
- 476 6. Raaz, U. et al. Segmental Aortic Stiffening Contributes to Experimental Abdominal Aortic Aneurysm Development. *Circulation*. **131**, 1783-1795 (2015).
- 7. van Disseldorp, E. M. J. et al. Influence of limited field-of-view on wall stress analysis in abdominal aortic aneurysms. *Journal of Biomechanics*. **49**, 2405-2412 (2016).
- 480 8. Miyatani, M. et al. Pulse wave velocity for assessment of arterial stiffness among people with spinal cord injury: a pilot study. *Journal of Spinal Cord Medicine*. **32**, 72-78 (2009).

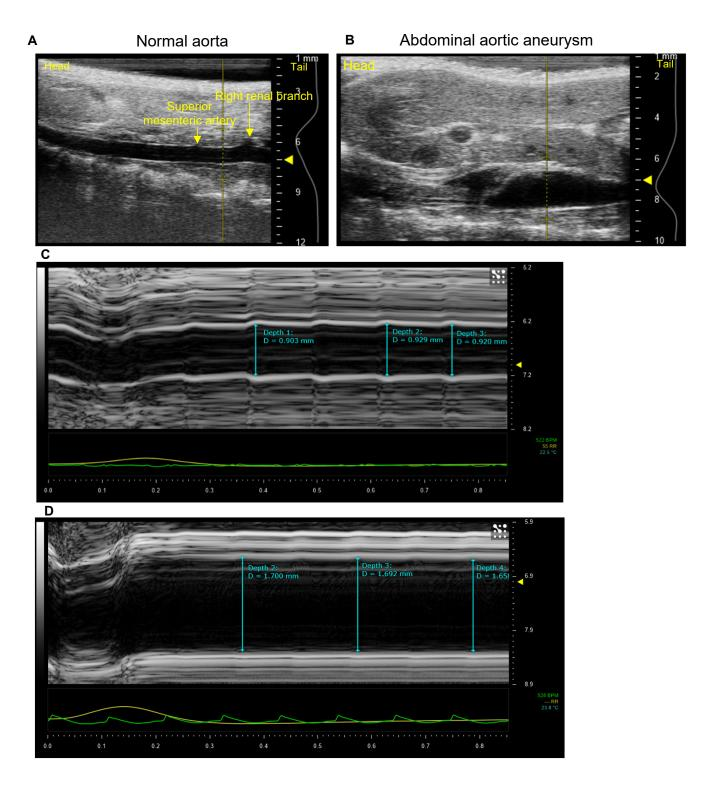
- 482 9. Sharma, N. et al. Deficiency of IL12p40 (Interleukin 12 p40) Promotes Ang II (Angiotensin
- 483 II)-Induced Abdominal Aortic Aneurysm. Arteriosclerosis, Thrombosis, and Vascular Biology. 39,
- 484 212-223 (2019).
- 485 10. Raaz, U. et al. Segmental Aortic Stiffening Contributes to Experimental Abdominal Aortic
- 486 Aneurysm Development. *Circulation*. **131**, 1783-1795 (2015).
- 487 11. Sharma, N. et al. Pharmacological inhibition of Notch signaling regresses pre-established
- 488 abdominal aortic aneurysm *Scientific Reports* (2019).
- 489 12. Bray, S.J. Notch signalling: a simple pathway becomes complex. *Nature Reviews*
- 490 *Molecular and Cell Biology.***7**, 678-89 (2006).
- 491 13. Hans, C.P. et al. Inhibition of Notch1 signaling reduces abdominal aortic aneurysm in
- 492 mice by attenuating macrophage-mediated inflammation. *Arteriosclerosis, Thrombosis and*
- 493 *Vascular Biology*. **32**, 3012-23 (2012).
- 494 14. Cheng, J., Koenig, S. N., Kuivaniemi, H. S., Garg, V., Hans, C. P. Pharmacological inhibitor
- of notch signaling stabilizes the progression of small abdominal aortic aneurysm in a mouse
- 496 model. *Journal of American Heart Association*. **3**, e001064 (2014).
- 497 15. Hans, C. P. et alTranscriptomics analysis reveals new insights into the roles of Notch1
- 498 signaling on macrophage polarization. *The Journal of Immunology*. **200**, 164.13 (2018).
- 499 16. Paraskevas, K. I. et al. Evaluation of aortic stiffness (aortic pulse-wave velocity) before
- and after elective abdominal aortic aneurysm repair procedures: a pilot study. *Open*
- 501 *Cardiovascular Medicine Journal.* **3**, 173-175 (2009).
- 502 17. Fortier, C., Desjardins, M. P., Agharazii, M. Aortic-Brachial Pulse Wave Velocity Ratio: A
- 503 Measure of Arterial Stiffness Gradient Not Affected by Mean Arterial Pressure. Pulse. 5, 117-
- 504 124 (2017).
- 505 18. Golledge, J. Abdominal aortic aneurysm: update on pathogenesis and medical
- treatments. *Nature Reviews Cardiology*. **16**(4), 225-242 (2019).
- 507 19. Choksy, S. A., Wilmink, A. B., Quick, C. R. Ruptured abdominal aortic aneurysm in the
- 508 Huntingdon district: a 10-year experience. Annals of the Royal College of Surgeons of England.
- 509 **81**, 27-31 (1999).

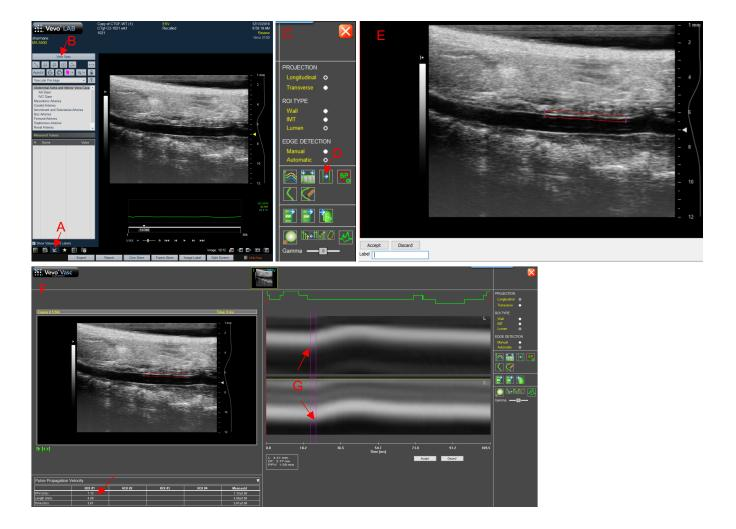
- 510 20. Luo, F., Zhou, X-L., Li, J-J., Hui, R-T. Inflammatory response is associated with aortic
- dissection. Ageing Research Reviews. **8**, 31-35 (2009)



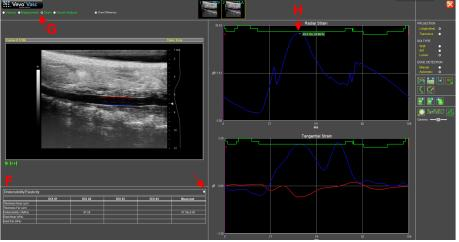


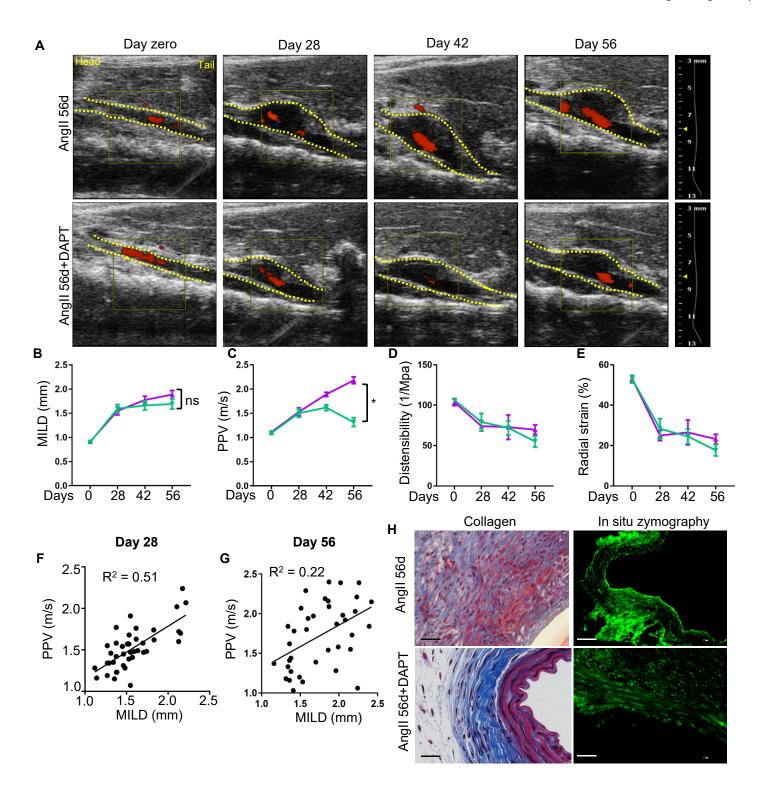












Name of Material/Equipment	Company	Catalog Number	Comments/Description
Angiotensin II	Sigma	A9525	
Apoe-/- mice	The Jackon lab	002052 - B6.129P2-Apoe <tm1unc>/J</tm1unc>	
clippers	WAHL	#1854	
Cotton swab	Q-tips		
DAPT	Sigma	D5942	
Depilatory cream	Nair	LL9038	
Electrode cream	Sigma Thermasonic	17-05	
Gel warmer	(Parker)	82-03 (LED)	
Heating pad	Stryker	T/pump professional	
Isoflurane	VetOne	Fluriso™	
Isoflurane vaporizer	Visualsonics	VS4244	
Lubricating ophthalmic ointment	Lacri-lube		
Osmotic pumps	Alzet	Model 2004	
Oxygen tank	Air gas		
Tranducer	Visualsonics	MS-400 or MS550D	
Ultrasonic gel	Parker	Aquasonic clear	
Ultrasound Imaging System	Visualsonics	Vevo 2100	
Vevo Vasc Software	Visualsonics		

TITLE:

Measurement of Pulse Propagation Velocity, Distensibility and Strain in Abdominal Aortic Aneurysm Mouse Model

3 4 5

1

2

AUTHORS AND AFFILIATIONS:

6

Neekun Sharma^{1,3*}, Zhe Sun^{1,2*}, Michael A. Hill^{1,2,3}, Chetan P. Hans^{1,2,3}

7 8 9

¹Division of Cardiovascular Medicine, University of Missouri, Columbia

²Medical Pharmacology and Physiology, University of Missouri, Columbia

10

³Dalton Cardiovascular Research Center, University of Missouri, Columbia

11 12

*These authors contributed equally.

13

14 Correspondence to:

15 Chetan P. Hans (HansCP@health.missouri.edu)

16

17 Email Addresses of Co-authors:

18 Neekun Sharma (sharmane@health.missouri.edu)

19 Zhe Sun (sunzh@missouri.edu)

20

(hillmi@missouri.edu)

21 22

KEYWORDS:

Michael A. Hill

Abdominal aortic aneurysm, animal models of human disease, pulse propagation velocity, distensibility, strain, aortic stiffness, in-vivo imaging

24 25 26

27

28

23

SUMMARY

Our manuscript describes a detailed protocol for using high frequency ultrasound imaging to measure luminal diameter, pulse propagation velocity, distensibility and radial strain on a mouse model of abdominal aortic aneurysm.

29 30 31

32 33

34

35

36 37

38

39

40

41

42

ABSTRACT

Abdominal aortic aneurysm (AAA) is defined as a localized dilation of the abdominal aorta that exceeds the maximal intraluminal diameter (MILD) by 1.5 times of its original size. Clinical and experimental studies have shown that small aneurysms may rupture, while a subpopulation of large aneurysms may remain stable. Thus, in addition to measurement of intraluminal diameter of the aorta, knowledge of structural traits of the vessel wall may provide important information to assess the stability of AAA. Aortic stiffening has recently emerged as a reliable tool to determine early changes in the vascular wall. Pulse propagation velocity (PPV) along with distensibility and radial strain are highly useful ultrasound-based methods relevant for assessing aortic stiffness. The primary purpose of this protocol is to provide a comprehensive technique for the use of ultrasound imaging system to acquire images and analyze the structural and functional properties of the aorta as determined by MILD, PPV, distensibility and radial strain.

INTRODUCTION

Abdominal aortic aneurysm (AAA) represents a significant cardiovascular disease characterized by a permanent localized dilation of the aorta exceeding the original vessel diameter by 1.5 times¹. AAA ranks among the top 13 causes of mortality in the United States². The progression of AAA is attributed to the degeneration of aortic wall and elastin fragmentation ultimately leading to aortic rupture. These changes in the aortic wall may occur without a significant increase in the maximal intraluminal diameter (MILD), thus suggesting that MILD alone is not sufficient to predict the severity of the disease³. Therefore, additional factors need to be identified to detect initial changes in the aortic wall, which may guide early treatment options. The overall goal of this protocol is to provide a practical guide for assessing aortic functional properties using ultrasound imaging as characterized by measurements of pulse propagation velocity (PPV), distensibility and radial strain.

A well characterized experimental model to study AAA, first described by Daugherty and colleagues, involves subcutaneous infusion of angiotensin II (AngII) via osmotic pumps in *Apoe*-/-mice⁴. Precise measurement of MILD using ultrasound imaging has been instrumental in characterizing AAA in this mouse model⁵. Although histological changes during the development of AAA have been extensively studied, changes in the functional properties of the vessel wall such as aortic stiffness have not been well characterized. This protocol emphasizes the use of high-frequency ultrasound in combination with the sophisticated analyses as powerful tools for studying the temporal progression of AAA. Specifically, these approaches allow us to assess the functional properties of the vessel wall as measured by PPV, distensibility and radial strain.

Recent clinical studies in human subjects with AAA, as well as in the murine elastase-induced AAA model, suggest a positive correlation between aortic stiffness and aortic diameter^{6, 7}. PPV, an indicator of aortic stiffness, is accepted as an excellent measurement for quantifying changes in stiffness in vessel wall^{6, 8}. PPV is calculated by measuring the transit time of the pulse waveform at two sites along the vasculature, thus providing a regional assessment of aortic stiffness. We have recently demonstrated that increased aortic stiffness as measured by PPV, and at the cellular level as determined using atomic force microscopy, positively correlates with aneurysm development9. Further, the literature suggests that aortic stiffness may precede aneurysmal dilation and thus may provide useful information about regional intrinsic properties of the vessel wall during development of AAA¹⁰. Similarly, distensibility and strain measurements are the quantification tools to measure earlier changes of arterial fitness. Healthy arteries are flexible and elastic, whereas with increased stiffness and less elasticity, distensibility and strain is decreased. Here, we provide a practical guide and step by step protocol for the use of a highfrequency ultrasound system to measure MILD, PPV, distensibility and radial strain in mice. The protocol provides technical approaches that should be used in conjunction with basic information provided by manuals for specific ultrasound imaging instruments and the accompanying video tutorial. Further, we provide example images and measurements taken from our studies of pharmacological approaches for preventing experimental AAA. Importantly, in our hands the described imaging protocol provides reproducible and accurate data that appear valuable in the study of the development and progression of experimental AAA.

Formatted: Strikethrough

To further demonstrate the utility of ultrasound imaging, we provide example images and measurements taken from our own studies aimed at using pharmacological approaches for preventing experimental AAA. ASpecifically, notch signaling ishas been proposed to be involved in multiple aspects of vascular development and inflammation. 11 Using the gene haploinsufficiency and pharmacologic approaches, we have previously demonstrated that Notch inhibition reduces the development of AAA in mice by preventing infiltration of macrophages at the site of vascular injury 12-14. For thise current article, using the pharmacological approach for notch inhibition we focus on validated the correlation the relationship of between a ortic stiffness with and the factors of relating to AAA stability in a mouse model using a potent pharmacologic inhibitor of Notch signaling and mimicking the clinical settings. Our These studies concluded illustrate that Notch inhibition reduces the aortic stiffness, which is a measure of AAA progression. Applications of Notch inhibitors in animal models of AAA provides a new perspective for novel target discovery to prevent or delay AAA formation (manuscript accepted in Scientific Reports).

PROTOCOL

86

87

88

89

90

91

92

93 94

95

96

97

98

99

100 101 102

103

104

105

106 107

108

111

112 113

114

115 116

117 118

119

120 121

122

123 124

125 126

127

The protocol for handling of mice and ultrasound imaging was approved by the University of Missouri Institutional Animal Care and Use Committee (animal protocol number 8799) and was conducted according to AAALAC International Standards.

1. Equipment set up and preparation of mice

1.1. Equipment set up

109 110

1.1.1. Turn on the ultrasound instrument, ultrasonic gel warmer and the heating pad.

1.1.2. Open the ultrasound program and enter the study name and descriptive information for each mouse.

1.1.3. Select the application as General Imaging.

1.1.4. Choose the appropriate transducer for abdominal imaging (Figure 1B,C). In this experiment, MS400 transducer is used.

1.1.5. Ensure anesthesia isoflurane and oxygen levels are adequate for each experimental session.

1.1.6. Clean the ultrasound animal imaging platform.

1.2. Mouse Preparation

Formatted: Indent: First line: 0.5"

Formatted: Strikethrough

Formatted: Underline, Strikethrough

Formatted: Underline, Strikethrough, Highlight

Formatted: Underline, Strikethrough

Formatted: Underline Formatted: Strikethrough

Commented [A1]: I have highlighted steps which will be used for filming purpose. Please check and approve/edit.

Please ensure that the highlighting is no more than 2.75 pages including headings and spacings and is in line with the title of the manuscript.

Commented [A2R1]: The highlighted portion is less than 2.75 pages and is according to JOVE guidelines.

1.2.1. Place the mouse cage on top of a heating pad (36.5 to 38.5 °C). 1.2.2. Gently hold the mouse by its tail and place in the oxygen-filled isoflurane chamber. 1.2.3. Direct the isoflurane and oxygen flow to the induction chamber. 1.2.4. Turn on the isoflurane vaporizer and set the isoflurane level to 1-2% vol/vol. Turn on the oxygen tank pressure to 1-2 L/min. 1.2.5. After ~ 2 min, confirm the adequate depth of anesthesia by the absence of withdrawal reflexes upon pinching the foot pad of the mouse. 1.2.6. Next, turn off the induction chamber supply branch and turn on the branch directed to the anesthesia nose cone. 1.2.7. Transfer the mouse from the induction chamber to the ultrasound imaging stage and position the anesthesia cone over the nose of the animal. 1.2.8. Tilt the animal imaging platform around 10° to the lower right corner for optimal scanning (Figure 1B). 1.2.9. Put one drop of sterile ophthalmic solution in both eyes of mice to prevent drying under anesthesia. 1.2.10. Position the mouse in the supine position with its nose inserted into the anesthesia cone. 1.2.11. Apply electrode gel to all four paws using a cotton swab and tape the paws to the copper leads on the animal imaging platform for electrocardiogram readings (Figure 1C). 1.2.12. Use clippers to shave hair at the imaging site and then apply depilatory cream to remove remaining fur. Leave for less than 1 min. 1.2.13. Gently wipe off the cream and hair with a damp paper towel. 1.2.14. Monitor the breathing and ensure that heart rate is maintained between 450-550 beats/min. If below this level, reduce the isoflurane flow and wait until the heart rate recovers. 1.2.15. Apply prewarmed ultrasonic gel (37 °C) to the prepared skin site and attach the transducer to its holder and lower down until it touches the gel (Figure 1C). 2. Ultrasound Imaging of Abdominal Aorta 2.1. Position the transducer horizontally i.e., perpendicular to the midline of the mouse.

2.2. Smooth the ultrasonic gel and remove bubbles using the wood stick of a cotton swab.

173

174

175 176

177 178

179

184 185 186

191 192 193

202 203 204

209

210 211 212

213 214 215 2.3. Lower the transducer and place 0.5 - 1 cm below the diaphragm after touching the gel. Now start to observe the images.

2.4. Visualize the abdominal aorta in the short axis view of the B-mode (Figure 1C).

NOTE: B-mode is the default and most effective mode to anatomically locate the aorta and position the transducer. The abdominal aorta is identified by the presence of pulsatile flow using color Doppler and power Doppler modes in the short axis (i.e., the circumferential cross-section of the aorta). Adjust the micromanipulators on the animal stage and the transducer to bring the cross section of the aorta to the center of the image.

2.5. Gently rotate the transducer 90° clockwise, and slowly adjust the x-axis micromanipulator knob to visualize the aorta in long axis view (longitudinal section of the aorta).

NOTE: In many cases, gastro-intestinal gases may interfere with the image, or the aorta may not be at the optimal angle to allow a clear long axis view. Adjust the angle of the transducer slowly and horizontally until an acceptable long axis view is obtained. If problems persist, elevate the transducer, check for air bubbles under the transducer, slightly adjust the tilting angle of the animal stage, reapply gels, and repeat the steps from (i) again.

- 2.6. Set the focus zone and depth at the region of the aorta using the Focus Zone and Focus Depth toggles, respectively. Adjust the time gain compensation slider manually to darken the lumen of the aorta to achieve an optimal contrast of the aorta wall.
- 2.7. Adjust the y-axis manipulator to visualize the branching points of the superior mesenteric and the right renal arteries. Use the right renal artery as a landmark to capture image of the suprarenal aorta (Figure 2A).
- 2.8. Record at least 100 frames of B-mode images on the suprarenal aorta.
- 2.9. Press cinestore to save the B-mode images.
- 2.10. Press M-mode button on the instrument keyboard to enable M-mode recording. Roll the cursor ball to bring the yellow indicator line to a normal aorta sections with clear vessel wall image, or to the sections where maximal diameter of aneurysm is observed.
- 2.11. Press the SV/gate toggle and adjust the cursor ball to ensure that vessel walls are included in the measurement bracket. Press update to record M-mode measurements and press cinestore to capture (Figure 2A,B).

NOTE: Maximal diameter of the aneurysm may not be in the same imaging plane as the optimal long axis view of the aorta. Adjust the x-axis manipulator knob slightly for each M-mode measurement to ensure that the MILD of each section is captured.

Commented [A3]: This is not showing the b mode.

Commented [A4R3]: We fixed it.

2.12. To obtain ECG-gated Kilohertz Visualization (EKV) images, press the **B-mode** button to go back to B-mode recording.

NOTE: If the images are not sharp, adjust the x-axis manipulator to achieve the sharpest image of upper wall of the lumen over a section length (i.e. >6 mm).

2.13. Press **Physio Settings** button on the keyboard and select **Respiration Gating**. Adjust the gating **Delay** and **Window** manually to record the data only during the flatter parts of the respiration wave. The recording sections will be shown as colored blocks on the tracing of the respiration wave.

NOTE: Without adjustment of the respiration gating, the EKV images will be blurred due to the normal movement of animal during breathing.

2.14. Press **EKV button** to enable the EKV mode. In the appropriate menu, select **Standard Resolution** and **frame rate 3000 or higher**. Select proceed to record **EKV images**. Press **cinestore** to save the images. Use EKV mode image to obtain measurements of pulse propagation velocity (PPV), distensibility and radial strain.

NOTE: EKV recording may fail if there are abnormal fluctuations in respiration, animal is respiring too rapidly, or frame rates settings are too high. In those case, set the frame rate lower and wait for the animal respiration to stabilize. Setting the frame rate at 3000 is usually appropriate for both mice and rats.

3. Post-imaging steps

3.1. Gently wipe the ultrasonic gel from the abdominal area of the mouse with a paper towel moistened with warm water.

3.2. Place the mouse back in its home cage on a heating pad.

3.3. Turn off the isoflurane machine, clean the animal imaging platform and transducer with damp wipes.

3.4. Transfer the image data collected during the ultrasound scan to the hard drive.

3.5. Turn off the ultrasound instrument.

3.6. After the mouse recovers from anesthesia and is alert, remove the heating pad and return the cage to the animal housing rack.

4. Analysis of abdominal aortic images

- 4.1. Analysis of M-mode images to measure MILD
- 4.1.1. Open the ultrasound program and enter the study name and descriptive information for each mouse.
- 4.1.2. Open the ultrasound data in the analysis software and open the M-mode image and pause the heartbeat.
- 4.1.3. Click on Measurements.

4.1.4. Select the **vascular package** from the drop-down options. Click on **Depth** and draw a line across the aortic lumen extending from inner wall to wall (**Figure 2**CA,DB).

NOTE: For consistency, the measurements should be taken at the systolic phase of the cardiac cycle when the aorta is maximally expanded. Draw_three lines across three different heartbeats to get the obtain accurate and average measurements of MILD. In AAA, the measurements are taken at the maximal dilatation of the aorta. It is also advisable to fast the animals 4-6 h prior to collecting images to avoid interference from bowel motility and ensure image clarity.

4.1.5. Draw three lines Measure the MILD across three different heartbeats to measure the MILD and calculate the average measurements (Figure 26,D).

- 4.2. Analysis for pulse propagation velocity (PPV)
- 4.2.1. Open the EKV image and pause the heartbeat.
- 4.2.2. Open a new window on the analysis software (Vevo Vac) by clicking on the name icon.
- 4.2.3. Click on the **PPV option** (arrow in Figure 3D). A small window will further appear with the image of the aorta.
- 4.2.4. Draw a rectangular box by clicking on the topupper vessel wall and dragging the pointer for about 4 mm covering both the walls of the suprarenal aorta.

NOTE: Keep the length of the box consistent (~4 mm) for all the images. The user can adjust rectangular box by rotating to align the box and selecting the line then dragging to a new position on the vessel being analyzed to obtain the most appropriate and clear inflection of the pulse wave. The vertical lines of data from the rectangle will be displayed and identified as the Left (top image) and Right (bottom image) on the ROI. For a better visualization of the inflection of the pulse wave, it is sometimes useful to the draw box only on the upper wall as shown in **Figure 3**. The software will automatically calculate the PPV (m/s). However, it's always better to manually adjust the purple lines to set the exact inflection point on the pulse waves and PPV will change accordingly.

Commented [A5]: Please check the figure number.

Commented [A6R5]: Fixed.

Commented [A7]: How is this done?

Commented [A8R7]: The details have been provided.

Formatted: Not Highlight

Formatted: Not Highlight

Formatted: Not Highlight

Commented [A9]: How is this done?

Commented [A10]: How?

Commented [A11R10]: Fixed.

4.2.5. Finally, select the **Accept** command to save the PPV values. Export the figures and the data to the data storage drive.

4.3. Analysis for distensibility and radial strain

4.3.1. Open the EKV image and pause the heartbeat.

4.3.2. Click on the software icon The software will open a new window.

4.3.3. Click on the "trace new ROI" and draw a rectangular box on the both walls of the vessel. The software will automatically trace the upper and lower walls of the vessel. The user can adjust the trace to align on the wall by clicking on green points (Figure 4A, B).

4.3.4. Now "Accept" the trace. The software will calculate the distensibility (1/Mpa) in the selected ROI.

4.3.5. For the radial strain measurement, select the appropriate strain option from the menu bars on the top left. The images for radial strain and tangential strain will open.

4.3.6. Obtain the value for radial strain (%) by moving the cursor on the peak of the curve. Export the data as images or in video format (Figure 4A,B).

REPRESENTATIVE RESULTS

Representative M-mode images of the normal and aneurysmal abdominal aorta from mice are shown in Figure 2A and 2B, respectively. The suprarenal abdominal aorta is identified by its location next to right renal artery and the superior mesenteric artery (Figure 2A). Representative images used for the calculation of MILD, at three different heartbeats of the systolic cardiac cycle, in normal and aneurysmal aorta are shown in Figure 2C and 2D, respectively. In the situation where an aortic aneurysm has developed, the luminal diameter is determined by drawing a perpendicular yellow line between the two inner edges of the lumen at the area of maximal dilation (Figure 2B). Three independent measurements are typically averaged to determine an accurate intraluminal diameter.

Representative EKV images of the abdominal aorta used in analysis of PPV are shown in Figure 3. PPV is calculated by drawing a rectangular box on the luminal wall of suprarenal aorta (Figure 3E) and adjustment of the purple vertical lines of data obtained from the rectangular box (Figure 3F). The purple lines should be adjusted to set the inflection point of the pulse waves. Representative EKV images of the abdominal aorta suitable for analysis of distensibility and radial strains are shown in Figure 4. Distensibility and radial strain are calculated by tracing the luminal walls of the suprarenal aorta as shown in Figure 4E. The value for distensibility (1/MPa) is obtained by choosing the distensibility/elasticity option from drop down menu of the box (red arrow, Figure 4F). The radial strain (%) is obtained by choosing the radial strain option (Figure 4G) and moving the cursor to the peak of the radial strain graph (Figure 4H).

In our own studies, wWe have validated the significance of PPV in the AnglI-induced mouse model of AAA and further examined the therapeutic potential of a Notch inhibitor (N-[N-(3,5difluorophenacetyl)-L-alanyl]-(S)-phenylglycine t-butyl ester; DAPT) on the progression and stability of pre-established AAA. Specifically, all these aneurysm studies were performed on 8-10 weeks old Apoe^{-/-} male mice following infusion of AngII by published protocols^{4, 12}. At day 28 of AnglI infusion, mice were randomly divided into two groups and were administered vehicle or DAPT (10 mg/kg) until sacrifice at day 56¹². Transabdominal ultrasound imaging showed a progressive increase in the MILD, PPWV, and a decrease in distensibility and radial strain in response to AnglI at day 28 (Figure 5A-E). AnglI infusion marginally increased MILD from day 28 to 56 and DAPT did not significantly change MILD compared to AnglI alone (Figure 5A and 5B). However, PPV increased progressively with AnglI infusion at from day 28 to day 56 and DAPT significantly decreased further increases in PPV at day 56 (Figure 5C). Distensibility and radial strains, parameters to assess the elasticity of the vessel wall were decreased with AngII infusion while DAPT showed no significant effect (Figure 54D and 54E). It is important to appreciate that PWV correlated strongly with MILD at day 28 (R²=0.51, Figure 5F), whereas at day 56, the correlation was relatively weak (R²=0.22) (Figure 5G). Aortic stiffness in AAA is primarily associated with changes in aortic wall architecture. Histologically, AnglI infusion increased collagen degradation and proteolytic activity in the medial layer of the aorta (Figure 5H, top row). DAPT treatment minimized such changes in the ECM degradation (Figure 5H, bottom row).

FIGURE LEGENDS

348

349

350

351

352

353

354

355 356

357

358

359

360 861

362

363

364

365

366

367 368

369

370

371

372

373

374 375

376

377

378

379

380 381

382

383

384

385

386

387 388

389

390

391

Figure 1: Set up of the instrument. (A) Overall view of the ultrasound machine along with induction chamber for anesthesia and gel warmer. (B) Close up view of the imaging platform and the transducer system. (C) The view of the transducer placement while capturing short axis image of the abdominal aorta.

Figure 2: Analysis of M-mode images for obtaining maximal intraluminal diameter (MILD). The M-mode images of normal aorta (A) and aorta with abdominal aortic aneurysm (B) from mice are shown. (C) and (D), MILD drawn at systolic phase of the cardiac cycle in the suprarenal aorta of normal mice (C) and mice with AAA (D). Measurements at three different heartbeats are taken as shown and the average value is calculated.

Figure 3: Analysis of EKV images for obtaining pulse propagation velocity (PPV). EKV images collected from normal mouse aorta. Analysis is done by clicking on measurements (A) and the software icon (B). A new window will appear with the icons on the right side, as shown in C. Now, click on PPV (D) and again, a small window will appear (E). Draw a rectangular box on the upper wall of the lumen as shown in E and click accept. The PPV value will be obtained as shown in F (arrow). The purple lines is adjusted to set the inflection point of the pulse waves (G).

Figure 4: Measurement of distensibility and radial strain. EKV images collected from normal mouse aorta. Analysis is done by clicking on measurements (A) and the software icon (B). A new window will appear with the icons on the right side, as shown in C. Now, click on trace new ROI (D), a new window will appear with traces on the upper and the lower wall of the lumen as shown

Commented [A12]: Are figure 2, 3 4 not from your own study? If not please include citations.

Commented [A13R12]: All these images belong to our studies, the sentences have been modified.

Commented [A14]: In the introduction section, please include the significance of using a notch inhibitor as a potential therapeutic for AAA

Commented [A15R14]: The request information is now provided.

Commented [A16]: Please expand.

Commented [A17R16]: Fixed.

Commented [A18]: Is this Figure 5?

Commented [A19R18]: Apologies for typo, it's fixed now.

Commented [A20]: Please check the figure number

Commented [A21R20]: Corrected.

Commented [A22]: The figure resolutions are not great. Please upload high resolution figures in .psd, .ai, etc.

 $\label{lem:commented} \textbf{Commented [A23R22]:} \ \mbox{We have uploaded high resolution images.}$

Commented [A24]: Please do not show the commercial tem Vevo Vac in the figures.

Commented [A25R24]: Fixed.

Commented [A26]: Please do not show the commercial tem Vevo Vac in the figures.

Commented [A27R26]: Fixed.

in **E** and click accept. The value for distensibility will be obtained in table as show in the **F**. For strain, click on strain (**G**). The window will show the radial strain value (%, green highlighted box), as the cursor is placed on the peak of the radial strain graph (**H**).

Figure 5. PPV correlates with structural traits of aorta in the established AAA. (A) Representative transabdominal ultrasound images showing the MILD at day 0, 28, 42 and 56 of indicated experimental groups in Apoe^{-/-} mice. DAPT was started at day 28. Dotted yellow lines outline the lumen. (B) Quantification of MILD in the indicated groups (purple and green color shows AngII + vehicle and AngII + DAPT treated mice respectively (n=16-18). (C, D and E) PPV, distensibility and radial strain at various days of AngII and DAPT treatments (n=8). (F and G), Graphs showing Pearson's correlation between PPV and MILD at day 28 (F) and day 56 (G). (H) Representative histological images for collagen staining (stained with trichrome and seen as blue staining) and proteolytic activity by in situ zymography with or without DAPT treatment at day 56. Tukey multiple comparisons test was used for data analysis. *P<0.05; ns = non-significant. Scale 50 µm in H. This figure is adapted from 'Pharmacological inhibition of Notch signaling regresses preestablished abdominal aortic aneurysm' by Sharma et al (2019), Scientifc Reports** (SREP-19-16491B; permission pending).

Table of Materials:

DISCUSSION

Ultrasound imaging provides a powerful technique for determining functional properties of the aorta through measurements of PPV, distensibility and radial strain. These measurements are particularly instructive for studying mouse models of AAA and the in vivo approach allows for collection of longitudinal data that is potentially important to understanding temporal development of the aortic pathology. Specifically, measurements of in vivo aortic stiffness are determined locally in the abdominal aorta by PPV, distensibility and radial strain by analyzing EKV data and are considered as an independent risk factor for AAA instability¹⁵. The techniques described in these protocols are relatively straight forward and take only 8-10 min to obtain image sets from one mouse. All images should preferably be collected by a single operator using well-defined and consistent landmarks to generate reproducible and precise data.

There are potential factors which requires technical expertise for the applications of these tools. For example, firstly, PPV may not solely reflect the degree of AAA development in the local arterial wall because it is an indirect measure of regional arterial stiffness. Secondly, it can be difficult to accurately measure PPV if the intimal wall is damaged. Third, it can be challenging to obtain sharp resolution images without expertise in operating the instrument. Some of these concerns have been addressed in tems where speckle noise and artifacts are reduced, while preserving and enhancing data acquisition for small animal studies.

The focus of techniques used in the past (Doppler, microangiography, magnetic resonance imaging) to determine aortic stiffness were limited to two-dimensional images. PPV calculated

Commented [A28]: Please mention which color corresponds to what group? What

Commented [A29R28]: Fixed.

Commented [A30]: Figure has PWV instead. Please keep the terms consistent. Please expand in the figure legend.

Commented [A31R30]: We have revised the terms.

Formatted: Font: Not Bold

Commented [A32]: Please include the citation here. Please upload the reprint publication upon acceptance of the manuscript. We will have to hold off this publication until the parent manuscript is published.

Please also include the citation in the reference section upon acceptance.

Commented [A33R32]: We have applied for the permission to reprint.

 $\label{lem:commented A34: This is incomplete. Please include all materials used for the experiment detailed in the protocol. E.g. depilatory cream, Q-tips, etc.$

Commented [A35]: We cannot have commercial terms in the manuscript. Please use generic terms instead.

Commented [A36R35]: Fixed.

from the ultrasound imaging has been emerging as a reliable and reproducible method to determine aortic stiffness and seems to be independent of arterial pressure ^{9, 16}. It is important to note that the prevailing definition of AAA using maximal diameter as a standard index does not always reliably correlate with clinical observations. For instance, small aneurysms may rupture while some large aneurysms tend to remain stable ¹⁷⁻¹⁹. Aortic stiffening is an early change generating aortic wall stress that triggers aneurysmal growth, and remodeling ¹⁰ and has been strongly correlated with Mmp2 and Mmp9 in mouse models of AAA ¹⁰. Thus, in addition to the diameter of the aorta, functional analyses may provide important information to assess the progression and stability of AAA.

Using these protocols, we have examined the therapeutic potential of a potent pharmacological Notch inhibitor (2S-N-[(3,5-Difluorophenyl) acetyl]-L-alanyl-2-phenylglycine 1,1-dimethylethyl ester; DAPT) on the progression and stability of pre-established AAA using an AnglI-induced mouse model of AAA. Transabdominal ultrasound imaging showed a progressive increase in the MILD, PWV, and a decrease in distensibility and radial strain in the Apoe-/- mice in response to AnglI than controls at day 28. No further increase in MILD was observed beyond day 28 till day 56 (Figure 5). However, PPV increased progressively and was significantly higher at day 56 compared to day 28. With the inhibition of Notch signaling by DAPT, MILD mice was not significantly different from AnglI alone at day 56. Interestingly, DAPT prevented further increase in PPV such that it was significantly lower than AngII at day 56 (Figure 5C). DAPT treatment did not significantly affect distensibility or radial strain (Figure 5D and E). Interestingly, PPV correlated strongly with MILD at day 28 (R2=0.51), whereas at day 56, the correlation was relatively weak (R²=0.22; Figure 5F). These changes in the aortic stiffness were reflected in the increased collagen degradation and proteolytic activity with AngII and the attenuation by DAPT (Figure 5H). This example study highlights the potential value of ultrasound-based aortic stiffness measurments in understanding the time-course and predictability of both AAA progression and stability.

Further, the ultrasound based approach appears valuable in assessing the potential role for pharmacological interventions, particularly in stages that are likely to be independent of changes in intra-luminal diameter (i.e. beyond expectation for actual regression). In summary, detailed understanding and usage of such technology will benefit in evaluating the prognosis of AAA at an early stage of the disease for effective therapeutic interventions.

ACKNOWLEDGMENTS

This work was supported by R01HL124155 (CPH) and funding from the Research Institute at the University of Missouri to CPH.

DISCLOSURES

The authors have nothing to disclose.

REFERENCES

1. Wanhainen A. How to Define an Abdominal Aortic Aneurysm — Influence on Epidemiology and Clinical Practice. *Scandinavian Journal of Surgery*. 2008;97:105-109.

- 480 2. Benjamin EJ, et al. Heart Disease and Stroke Statistics — 2018 Update: A Report From the 481 American Heart Association. Circulation. 2018;137:e67-e492.
- Xu J and Shi G-P. Vascular wall extracellular matrix proteins and vascular diseases. 482
- 483 Biochimica et biophysica acta. 2014;1842:2106-2119.
- 484 Daugherty A, Manning MW and Cassis LA. Angiotensin II promotes atherosclerotic
- lesions and aneurysms in apolipoprotein E-deficient mice. J Clin Invest. 2000;105:1605-12. 485
- 486 Au - Sawada H, et al. Ultrasound Imaging of the Thoracic and Abdominal Aorta in Mice to Determine Aneurysm Dimensions. JoVE. 2019:e59013. 487
- Raaz U, et al. Segmental Aortic Stiffening Contributes to Experimental Abdominal Aortic 488 489 Aneurysm Development. Circulation. 2015;131:1783-1795.
- 490 van Disseldorp EMJ, et al. Influence of limited field-of-view on wall stress analysis in 491 abdominal aortic aneurysms. Journal of Biomechanics. 2016;49:2405-2412.
- 492 Miyatani M, et al. Pulse wave velocity for assessment of arterial stiffness among people 493 with spinal cord injury: a pilot study. J Spinal Cord Med. 2009;32:72-78.
- 494 Sharma N, et al. Deficiency of IL12p40 (Interleukin 12 p40) Promotes Ang II (Angiotensin
- 495 II)-Induced Abdominal Aortic Aneurysm. Arteriosclerosis, thrombosis, and vascular biology.
- 496 2019;39:212-223.
- Raaz U, et al. Segmental Aortic Stiffening Contributes to Experimental Abdominal Aortic 497 10. 498 Aneurysm Development. Circulation. 2015;131:1783-1795.
- 499 Bray SJ. Notch signalling: a simple pathway becomes complex. Nat Rev Mol Cell Biol. 500 2006:7:678-89.
- 501 Hans CP, et al. Inhibition of Notch1 signaling reduces abdominal aortic aneurysm in mice by attenuating macrophage-mediated inflammation. Arterioscler Thromb Vasc Biol.
- 502
- 503 2012;32:3012-23.
- 504 Cheng J, Koenig SN, Kuivaniemi HS, Garg V and Hans CP. Pharmacological inhibitor of 505 notch signaling stabilizes the progression of small abdominal aortic aneurysm in a mouse 506 model. J Am Heart Assoc. 2014;3:e001064.
- 507 Hans CP, et al. Transcriptomics analysis reveals new insights into the roles of Notch1 508 signaling on macrophage polarization. The Journal of Immunology. 2018;200:164.13.
- Paraskevas KI, et al. Evaluation of aortic stiffness (aortic pulse-wave velocity) before and 509
- 510 after elective abdominal aortic aneurysm repair procedures: a pilot study. Open Cardiovasc
- 511 *Med J.* 2009;3:173-175.
- Fortier C, Desjardins MP and Agharazii M. Aortic-Brachial Pulse Wave Velocity Ratio: A 512
- 513 Measure of Arterial Stiffness Gradient Not Affected by Mean Arterial Pressure. Pulse.
- 514 2017;5:117-124.
- 515 Golledge J. Abdominal aortic aneurysm: update on pathogenesis and medical 17.
- 516 treatments. Nature Reviews Cardiology. 2018.
- 517 Choksy SA, Wilmink AB and Quick CR. Ruptured abdominal aortic aneurysm in the
- 518 Huntingdon district: a 10-year experience. Annals of the Royal College of Surgeons of England.
- 519 1999;81:27-31.

523

520 Luo F, Zhou X-L, Li J-J and Hui R-T. Inflammatory response is associated with aortic 521 dissection. Ageing Research Reviews. 2009;8:31-35.

Formatted: EndNote Bibliography, Left



Vineeta Bajaj <vineeta.bajaj@jove.com>

Fwd: Scientific Reports: Decision letter for SREP-19-16491B

Hans, Chetan P. <hanscp@health.missouri.edu>
To: Vineeta Bajaj <vineeta.bajaj@jove.com>
Cc: "Sharma, Neekun" <sharmane@health.missouri.edu>

Wed, Sep 11, 2019 at 7:41 AM

FYI

Chetan P. Hans Sent from my iPhone

Begin forwarded message:

From: Journalpermissions < journalpermissions@springernature.com>

Date: September 11, 2019 at 5:44:44 AM CDT

To: "hanscp@health.missouri.edu" <hanscp@health.missouri.edu> **Cc:** Scientific reports <scientific.reports@springernature.com>

Subject: RE: Scientific Reports: Decision letter for SREP-19-16491B

Dear Chetan,

Thank you for your request. You are welcome to reuse material in new works created by yourself. If the Scientific Reports article is published prior to the new work, make sure to reference the original publication and if applicable, the CC license of your Sci Rep article.

Best wishes,

Oda

Oda Sigveland

Rights Executive

SpringerNature

The Campus, 4 Crinan Street, London N1 9XW,

United Kingdom

T +44 (0) 207 014 6851

http://www.nature.com

http://www.springer.com

http://www.palgrave.com

From: Hans, Chetan P. <hanscp@health.missouri.edu>

Sent: 05 September 2019 08:15 PM

To: Scientific reports <scientific.reports@springernature.com> **Subject:** RE: Scientific Reports: Decision letter for SREP-19-16491B

Hi Dr. Esfandiarei,

Thanks so much for accepting our manuscript in the Scientific Reports.

Can I request for the reprint permission of a part of the figures.

We are submitting a JOVE article "Measurement of Pulse Propagation Velocity, Distensibility and Strain in Abdominal Aortic Aneurysm Mouse Model"

I need to use a piece of data from the accepted article to demonstrate the utility of ultrasound imaging in a mouse model.

Thanks so much in advance.

Chetan P. Hans

Assistant Professor

School of Medicine - Cardiology &

Medical Pharmacology and Physiology

University of Missouri

Rm: 324B

Dalton Cardiovascular Research Center

134 Research Park Drive

Columbia, MO 65211

573-884-7225 ph

573-884-4232 fx

HansCP@health.missouri.edu

From: scientificreports@nature.com <scientificreports@nature.com>

Sent: Tuesday, August 27, 2019 4:40 AM

To: Hans, Chetan P. <hanscp@health.missouri.edu>

Subject: Scientific Reports: Decision letter for SREP-19-16491B

Dear Dr Hans,

We are delighted to accept your manuscript entitled "Pharmacological inhibition of Notch signaling regresses pre-established abdominal aortic aneurysm" for publication in Scientific Reports, a journal of the Nature Research family. Thank you for choosing to publish your work with us.

Licence to Publish

• The corresponding author of an accepted manuscript is required to complete an Open Access Licence to Publish on behalf of all authors; a link to the online portal through which you can submit this licence agreement will be sent in a separate email.

Article-processing charge

• If applicable, you will also receive a link to our payment application where you can provide your billing information and pay your article-processing charge (APC) via credit card or by requesting an invoice. Please see our FAQs page for further information about article processing charges.

Please note that your paper cannot be sent for typesetting to our production team until we have received the above information.

After we've prepared your paper for publication, you will receive an electronic proof for checking. At that point, please check the author list and affiliations to ensure that they are correct. For the main text, only errors that have been introduced during the production process or those that directly compromise the scientific integrity of the paper may be corrected at this stage. Please ensure that only one author communicates with us and that only one set of corrections is returned using the e-proofing tool. The corresponding (or nominated) author is responsible on behalf of all co-authors for the accuracy of all content, including spelling of names and current affiliations.

To ensure prompt publication, your proofs should be returned within two working days; please contact SciRep.Production@nature.com immediately if you wish to nominate a contributing author to receive the proofs on your behalf.

Acceptance of your manuscript is conditional on all authors' agreement with our publication policies (see http://www.nature.com/srep/policies/index.html). In particular, your manuscript must not be published elsewhere and there must be no announcement of this work to any media outlet until the publication date is confirmed. We will inform you by email as soon as your manuscript is scheduled for publication, which will be after we have received and approved your proof corrections. Advice about media relations is available from the Nature Research press office at press@nature.com.

Your article will be open for online commenting on the Scientific Reports website. You may use the report

facility if you see any comments which you consider inappropriate, and of course, you can contribute to discussions yourself. If you wish to track comments on your article, please register for this service by visiting the 'Comments' section in the full text (HTML) version of your paper.

A form to order reprints of your article is available at http://www.nature.com/reprints/author-reprints.html. To obtain the special author reprint rate, orders must be made within a month of the publication date. After that, reprints are charged at the normal (commercial) rate.

We look forward to publishing your article.

Best regards,

Mitra Esfandiarei Editorial Board Member Scientific Reports

- ** Nature Research journals encourage authors to share their step-by-step experimental protocols on a protocol sharing platform of their choice. Nature Research's Protocol Exchange is a free-to-use and open resource for protocols; protocols deposited in Protocol Exchange are citable and can be linked from the published article. More details can found at www.nature.com/protocolexchange/about.
- ** Visit the Springer Nature Editorial and Publishing website at www.springernature.com/editorial-and-publishing-jobs for more information about our career opportunities. If you have any questions please click here**

This email has been sent through the Springer Nature Tracking System NY-610A-NPG&MTS

Confidentiality Statement:

This e-mail is confidential and subject to copyright. Any unauthorised use or disclosure of its contents is prohibited. If you have received this email in error please notify our Manuscript Tracking System Helpdesk team at http://platformsupport.nature.com.

Details of the confidentiality and pre-publicity policy may be found here http://www.nature.com/authors/policies/confidentiality.html

Privacy Policy | Update Profile



ARTICLE AND VIDEO LICENSE AGREEMENT

Title of Article: High Frequency Olfrasound Evaluation of Abdominal April.

Aneurysms in Angiotensin II-Induced Mouse models

Neekun Sharma, The Sun, Michael A. Hill, Chetan P. Hans

Item 1: The Author elects to have the Materials be made available (as described at http://www.jove.com/publish) via:

Standard Access

The Author is NOT a United States government employee.

The Author is a United States government employee and the Materials were prepared in the

ARTICLE AND VIDEO LICENSE AGREEMENT

The Author is a United States government employee but the Materials were NOT prepared in the

course of his or her duties as a United States government employee.

course of his or her duties as a United States government employee.

Defined Terms. As used in this Article and Video License Agreement, the following terms shall have the following meanings: "Agreement" means this Article and Video License Agreement; "Article" means the article specified on the last page of this Agreement, including any associated materials such as texts, figures, tables, artwork, abstracts, or summaries contained therein; "Author" means the author who is a signatory to this Agreement; "Collective Work" means a work, such as a periodical issue, anthology or encyclopedia, in which the Materials in their entirety in unmodified form, along with a number of other contributions, constituting separate and independent works in themselves, are assembled into a collective whole; "CRC License" means the Creative Commons Attribution-Non Commercial-No Derivs 3.0 Unported Agreement, the terms and conditions of which can be found at: http://creativecommons.org/licenses/by-nc-

nd/3.0/legalcode; "Derivative Work" means a work based upon the Materials or upon the Materials and other preexisting works, such as a translation, musical arrangement, dramatization, fictionalization, motion picture version, recording, art reproduction, abridgment, condensation, or any other form in which the Materials may be recast, transformed, or adapted; "Institution" means the institution, listed on the last page of this Agreement, by which the Author was employed at the time of the creation of the Materials; "JoVE" means MyJove Corporation, a Massachusetts corporation and the publisher of The Journal of Visualized Experiments; "Materials" means the Article and / or the Video; "Parties" means the Author and JoVE; "Video" means any video(s) made by the Author, alone or in conjunction with any other parties, or by JoVE or its affiliates or agents, individually or in collaboration with the Author or any other parties, incorporating all or any portion

- of the Article, and in which the Author may or may not appear.
- 2. Background. The Author, who is the author of the Article, in order to ensure the dissemination and protection of the Article, desires to have the JoVE publish the Article and create and transmit videos based on the Article. In furtherance of such goals, the Parties desire to memorialize in this Agreement the respective rights of each Party in and to the Article and the Video.
- Grant of Rights in Article. In consideration of JoVE agreeing to publish the Article, the Author hereby grants to JoVE, subject to Sections 4 and 7 below, the exclusive, royalty-free, perpetual (for the full term of copyright in the Article, including any extensions thereto) license (a) to publish, reproduce, distribute, display and store the Article in all forms, formats and media whether now known or hereafter developed (including without limitation in print, digital and electronic form) throughout the world, (b) to translate the Article into other languages, create adaptations, summaries or extracts of the Article or other Derivative Works (including, without limitation, the Video) or Collective Works based on all or any portion of the Article and exercise all of the rights set forth in (a) above in such translations, adaptations, summaries, extracts, Derivative Works or Collective Works and(c) to license others to do any or all of the above. The foregoing rights may be exercised in all media and formats, whether now known or hereafter devised, and include the right to make such modifications as are technically necessary to exercise the rights in other media and formats. If the "Open Access" box has been checked in Item 1 above, JoVE and the Author hereby grant to the public all such rights in the Article as provided in, but subject to all limitations and requirements set forth in, the CRC License.



ARTICLE AND VIDEO LICENSE AGREEMENT

- 4. Retention of Rights in Article. Notwithstanding the exclusive license granted to JoVE in Section 3 above, the Author shall, with respect to the Article, retain the non-exclusive right to use all or part of the Article for the non-commercial purpose of giving lectures, presentations or teaching classes, and to post a copy of the Article on the Institution's website or the Author's personal website, in each case provided that a link to the Article on the JoVE website is provided and notice of JoVE's copyright in the Article is included. All non-copyright intellectual property rights in and to the Article, such as patent rights, shall remain with the Author.
- 5. Grant of Rights in Video Standard Access. This Section 5 applies if the "Standard Access" box has been checked in Item 1 above or if no box has been checked in Item 1 above. In consideration of JoVE agreeing to produce, display or otherwise assist with the Video, the Author hereby acknowledges and agrees that, Subject to Section 7 below, JoVE is and shall be the sole and exclusive owner of all rights of any nature, including, without limitation, all copyrights, in and to the Video. To the extent that, by law, the Author is deemed, now or at any time in the future, to have any rights of any nature in or to the Video, the Author hereby disclaims all such rights and transfers all such rights to JoVE.
- Grant of Rights in Video Open Access. This Section 6 applies only if the "Open Access" box has been checked in Item 1 above. In consideration of JoVE agreeing to produce, display or otherwise assist with the Video, the Author hereby grants to JoVE, subject to Section 7 below. the exclusive, royalty-free, perpetual (for the full term of copyright in the Article, including any extensions thereto) license (a) to publish, reproduce, distribute, display and store the Video in all forms, formats and media whether now known or hereafter developed (including without limitation in print, digital and electronic form) throughout the world, (b) to translate the Video into other languages, create adaptations, summaries or extracts of the Video or other Derivative Works or Collective Works based on all or any portion of the Video and exercise all of the rights set forth in (a) above in such translations, adaptations, summaries, extracts, Derivative Works or Collective Works and (c) to license others to do any or all of the above. The foregoing rights may be exercised in all media and formats, whether now known or hereafter devised, and include the right to make such modifications as are technically necessary to exercise the rights in other media and formats. For any Video to which this Section 6 is applicable, JoVE and the Author hereby grant to the public all such rights in the Video as provided in, but subject to all limitations and requirements set forth in, the CRC License.
- 7. Government Employees. If the Author is a United States government employee and the Article was prepared in the course of his or her duties as a United States government employee, as indicated in Item 2 above, and any of the licenses or grants granted by the Author hereunder exceed the scope of the 17 U.S.C. 403, then the rights granted hereunder shall be limited to the maximum

- rights permitted under such statute. In such case, all provisions contained herein that are not in conflict with such statute shall remain in full force and effect, and all provisions contained herein that do so conflict shall be deemed to be amended so as to provide to JoVE the maximum rights permissible within such statute.
- 8. Protection of the Work. The Author(s) authorize JoVE to take steps in the Author(s) name and on their behalf if JoVE believes some third party could be infringing or might infringe the copyright of either the Author's Article and/or Video.
- 9. Likeness, Privacy, Personality. The Author hereby grants JoVE the right to use the Author's name, voice, likeness, picture, photograph, image, biography and performance in any way, commercial or otherwise, in connection with the Materials and the sale, promotion and distribution thereof. The Author hereby waives any and all rights he or she may have, relating to his or her appearance in the Video or otherwise relating to the Materials, under all applicable privacy, likeness, personality or similar laws.
- 10. Author Warranties. The Author represents and warrants that the Article is original, that it has not been published, that the copyright interest is owned by the Author (or, if more than one author is listed at the beginning of this Agreement, by such authors collectively) and has not been assigned, licensed, or otherwise transferred to any other party. The Author represents and warrants that the author(s) listed at the top of this Agreement are the only authors of the Materials. If more than one author is listed at the top of this Agreement and if any such author has not entered into a separate Article and Video License Agreement with JoVE relating to the Materials, the Author represents and warrants that the Author has been authorized by each of the other such authors to execute this Agreement on his or her behalf and to bind him or her with respect to the terms of this Agreement as if each of them had been a party hereto as an Author. The Author warrants that the use, reproduction, distribution, public or private performance or display, and/or modification of all or any portion of the Materials does not and will not violate. infringe and/or misappropriate the patent, trademark, intellectual property or other rights of any third party. The Author represents and warrants that it has and will continue to comply with all government, institutional and other regulations, including, without limitation all institutional, laboratory, hospital, ethical, human and animal treatment, privacy, and all other rules, regulations, laws, procedures or guidelines, applicable to the Materials, and that all research involving human and animal subjects has been approved by the Author's relevant institutional review board.
- 11. JoVE Discretion. If the Author requests the assistance of JoVE in producing the Video in the Author's facility, the Author shall ensure that the presence of JoVE employees, agents or independent contractors is in accordance with the relevant regulations of the Author's institution. If more than one author is listed at the beginning of this Agreement, JoVE may, in its sole



ARTICLE AND VIDEO LICENSE AGREEMENT

discretion, elect not take any action with respect to the Article until such time as it has received complete, executed Article and Video License Agreements from each such author. JoVE reserves the right, in its absolute and sole discretion and without giving any reason therefore, to accept or decline any work submitted to JoVE. JoVE and its employees, agents and independent contractors shall have full, unfettered access to the facilities of the Author or of the Author's institution as necessary to make the Video, whether actually published or not. JoVE has sole discretion as to the method of making and publishing the Materials, including, without limitation, to all decisions regarding editing, lighting, filming, timing of publication, if any, length, quality, content and the like.

Indemnification. The Author agrees to indemnify JoVE and/or its successors and assigns from and against any and all claims, costs, and expenses, including attorney's fees, arising out of any breach of any warranty or other representations contained herein. The Author further agrees to indemnify and hold harmless JoVE from and against any and all claims, costs, and expenses, including attorney's fees, resulting from the breach by the Author of any representation or warranty contained herein or from allegations or instances of violation of intellectual property rights, damage to the Author's or the Author's institution's facilities, fraud, libel, defamation, research, equipment, experiments, property damage, personal injury, violations of institutional, laboratory, hospital, ethical, human and animal treatment, privacy or other rules, regulations, laws, procedures or guidelines, liabilities and other losses or damages related in any way to the submission of work to JoVE, making of videos by JoVE, or publication in JoVE or elsewhere by JoVE. The Author shall be responsible for, and shall hold JoVE harmless from, damages caused by lack of sterilization, lack of cleanliness or by contamination due to

the making of a video by JoVE its employees, agents or independent contractors. All sterilization, cleanliness or decontamination procedures shall be solely the responsibility of the Author and shall be undertaken at the Author's expense. All indemnifications provided herein shall include JoVE's attorney's fees and costs related to said losses or damages. Such indemnification and holding harmless shall include such losses or damages incurred by, or in connection with, acts or omissions of JoVE, its employees, agents or independent contractors.

- 13. Fees. To cover the cost incurred for publication, JoVE must receive payment before production and publication of the Materials. Payment is due in 21 days of invoice. Should the Materials not be published due to an editorial or production decision, these funds will be returned to the Author. Withdrawal by the Author of any submitted Materials after final peer review approval will result in a US\$1,200 fee to cover pre-production expenses incurred by JoVE. If payment is not received by the completion of filming, production and publication of the Materials will be suspended until payment is received.
- 14. Transfer, Governing Law. This Agreement may be assigned by JoVE and shall inure to the benefits of any of JoVE's successors and assignees. This Agreement shall be governed and construed by the internal laws of the Commonwealth of Massachusetts without giving effect to any conflict of law provision thereunder. This Agreement may be executed in counterparts, each of which shall be deemed an original, but all of which together shall be deemed to me one and the same agreement. A signed copy of this Agreement delivered by facsimile, e-mail or other means of electronic transmission shall be deemed to have the same legal effect as delivery of an original signed copy of this Agreement.

A signed copy of this document must be sent with all new submissions. Only one Agreement is required per submission.

CORRESPONDING AUTHOR

Name:	Chetan P. Hans
Department:	Division of Cardiovascular Medicine
Institution:	University of Misseuri
Title:	Assistant Professor
Signature:	Date: 07/01/2019

Please submit a signed and dated copy of this license by one of the following three methods:

- 1. Upload an electronic version on the JoVE submission site
- 2. Fax the document to +1.866.381.2236
- 3. Mail the document to JoVE / Attn: JoVE Editorial / 1 Alewife Center #200 / Cambridge, MA 02140